JOURNAL OF GEOPHYSICAL RESEARCH, VOL. 105, NO. A6, PAGES 12,667–12,674, JUNE 1, 2000

# Connecting the Sun and the solar wind: Source regions of the fast wind observed in interplanetary space

Richard Woo

Jet Propulsion Laboratory, California Institute of Technology, Pasadena

Shadia Rifai Habbal

Harvard-Smithsonian Center for Astrophysics, Cambridge, Massachusetts

**Abstract.** Highly sensitive radio occultation and white light measurements of path-integrated density have shown that the solar corona comprises three distinct morphological regions, streamer, quiet Sun, and polar coronal hole, which except for the streamer region, extend radially into interplanetary space from 1.15 $R_s$ to at least 30 $R_s$. In this paper we build on these results by comparing solar wind flow speeds observed at the same time as path-integrated density. Flow speeds are inferred from the Doppler dimming of O VI lines with the ultraviolet coronagraph spectrometer on the Solar and Heliospheric Observatory, while the simultaneous polarized brightness measurements of path-integrated density are from the High Altitude Observatory Mauna Loa Mk III K-coronameter. The comparison of global flow speed and density observations in 1997 produces three new results. First, it shows, that the three distinct morphological regions, identified earlier in density measurements, are present in the latitudinal profile of the flow speed in the corona. In particular, the flow speed measurements provide evidence for the quiet Sun as an additional source of fast wind. Second, the comparison shows that flow speed and density are anticorrelated in the solar corona. Third, it demonstrates that the Mk III pB measurements can readily serve as a proxy for velocity distribution in the outer corona. The extensive Mk III data set that spans nearly two solar cycles therefore provides the framework of near-Sun measurements with which connections with solar wind measurements in interplanetary space can be made. Specifically, we show that fast wind regions in the heliosphere, observed directly by Ulysses and Wind plasma measurements and remotely by Nagoya interplanetary scintillation measurements, map radially back to fast wind regions at the Sun identified by the Mk III data.

## 1. Introduction

Since the existence of the solar wind was confirmed by Mariner 2 [*Neugebauer and Snyder*, 1966], connecting the solar wind to the Sun has been one of the primary goals of solar wind research. As the number of interplanetary spacecraft has grown, so has our knowledge and understanding of the morphology of the three-dimensional heliosphere beyond 0.3 AU. By comparison, definitive measurements of the spatial distribution of plasma parameters in the solar corona have been rare.

Coronal holes have been regarded as the sources of the high-speed streams observed by interplanetary spacecraft for over 20 years [*Zirker*, 1977; *Hundhausen*, 1977]. When direct high-latitude measurements were eventually made by the Ulysses mission, it was further concluded that the observed fast wind at high latitude emanated solely from polar coronal holes and that it expanded superradially [e.g., *Gosling et al*., 1995; *Neugebauer*, 1999]. These major conclusions about the solar sources of the fast solar wind were not established by comparing the solar wind with velocity or magnetic field measurements in the corona because none were available. Instead, the observational connection was made by extrapolating back to the Sun the in situ velocity measurements of high-speed streams made beyond 0.3 AU and associating them with coronal holes deduced from soft X-ray or He I 1083 nm measurements and white light images of the corona [*Kreiger et al*., 1973; *Munro and Jackson*, 1977; *Bame et al*., 1993; *Gosling et al*., 1995].

New information on the morphology of coronal density (in this paper, density refers to path-integrated density) from 1.15 to 30 $R_s$ has now emerged as a result of radio occultation and white light measurements of high sensitivity and wide dynamic range [*Woo and Habbal*, 1999a, b]. By studying the latitudinal profiles for increasing heliocentric distance, polar coronal holes have been followed and found to expand radially rather than superradially as previously thought [*Munro and Jackson*, 1977]. Furthermore, these measurements have shown that polar coronal holes, the quiet Sun, and streamers comprise three distinct morphological regions of coronal density near solar minimum. Density in the quiet Sun region is a factor of 2–3 higher than that in the polar coronal hole, but the latitudinal density profile of both quiet Sun and polar coronal hole regions is radially preserved. The streamer region encompasses the heliospheric current sheet that evolves from coronal streamers within a few solar radii of the Sun. It is defined as the region in which the latitudinal density profile of the outer corona beyond 5 $R_s$ no longer matches the radially preserved density profile of the inner corona at 1.15 $R_s$ [*Woo and Habbal*,



Paper number 1999JA000255.
0148-0227/00/1999JA000255$09.00

1999b]. Instead, the latitudinal gradient rises steeply as it departs from a radial expansion.

Significant flow speed measurements of the corona have also been made. Radio occultation (mainly interplanetary scintillation (IPS)) measurements have probed solar wind velocity in the corona for many years [e.g., *Ekers and Little*, 1971; *Armstrong et al*., 1986; *Grall et al*., 1996] and hinted at the source regions of the solar wind [*Woo*, 1995; *Woo and Martin*, 1997]. However, it remained for ultraviolet Doppler dimming measurements to provide the definitive measurements of latitudinal variation because unlike the radio measurements, they were able to map a significant portion of the plane of the sky essentially at the same time [*Habbal et al*., 1997]. These measurements confirmed that streamer stalks are the sources of the slowest solar wind and that fast wind pervades the inner corona (see reviews by *Woo and Habbal* [1998, 1999c, and references therein]).

In this paper we build on the recent observational results by comparing simultaneous density and flow speed measurements in the inner corona. We show that the distribution of flow speed reflects the same morphological regions detected earlier in coronal density measurements alone. By comparing the latitudinal distribution of coronal density with the latitudinal distribution of flow speed in interplanetary space, we further demonstrate that in the absence of flow speed measurements in the inner corona, density can serve as a proxy for flow speed there, thus establishing the source regions of the fast solar wind observed in interplanetary space.

## 2. Simultaneous Flow Speed and Density Measurements in the Solar Corona

We compare solar wind flow speed inferred from measurements by the ultraviolet coronagraph spectrometer (UVCS) onboard the Solar and Heliospheric Observatory (SOHO) [*Kohl et al*., 1995] with density from polarized brightness (pB) measurements made by the HAO Mauna Loa Mk III K-coronameter [*Fisher et al*., 1981]. Since these data sets are of path-integrated measurements that were made simultaneously, they are affected by the same line-of-sight effects.

### 2.1. Solar Wind Flow Speed

Flow speed information has been inferred by *Habbal et al*. [1997] from the Doppler dimming UVCS measurements on SOHO for January 17–19, 1997, April 23–27, 1997, in the form of 94 km $s^{-1}$ contours. As explained by *Habbal et al*. [1997], a ratio of 2 of the intensities of the oxygen lines 1032/1037 Å measured by UVCS corresponds to an outflow velocity of 94 km $s^{-1}$, which is model-independent [*Habbal et al*., 1997].

The 94 km $s^{-1}$ contours represented by the solid white lines in Plates 1a (January 17) and 2a (April 27) are superimposed on the white light images of the SOHO Large-Angle and Spectrometric Coronagraph (LASCO) C2 coronagraph [*Brueckner et al*., 1995], which provides context for the UVCS observations. It is clear from Plates 1a and 2a that the heliocentric distance of the 94 km $s^{-1}$ contour varies as a function of latitude. Since radial distance to these contours is inversely proportional to flow speed, the contours also serve as an indicator of the latitudinal variation of the flow speed. We display radial distance in 5° increments of position angle (latitude is measured counterclockwise with respect to ecliptic north) in Plates 1b–1d and 2b–2d, choosing to plot radial distance increasing downward in order to depict a flow speed that increases upward. The measurement uncertainty in the position of the 94 km $s^{-1}$ contours is $\pm 0.05\ R_s$ in radial distance and 3° in latitude.

The measurements of January 1997 in Plate 1 show three distinct regions that can be identified in the slope of the radial distance profile or, equivalently, in the gradient of flow speed: (1) a flat slope covering ±22.5° about 180°, (2) a slowly declining profile between 112° and 150°, and (3) a very sharp decline toward the streamer stalk at position angles <112°. In the case of the data of April 1997 in Plate 2 the 94 km $s^{-1}$ velocity contour does not extend to high latitudes, and only the region of very sharp decline in the slope of the radial distance profile north and south of the streamer is evident. In section 2.2 we will use simultaneous Mk III density measurements to show that the three distinct regions in flow speed and their demarcations, summarized in Plates 1d and 2d, coincide with those identified previously by density measurements alone.

### 2.2. Density As a Proxy for Solar Wind Velocity

Three major morphological regions of the solar corona, polar coronal hole, quiet Sun, and streamer, have been identified by following the evolution of the latitudinal profile of path-integrated density with increasing heliocentric distance from 1.15 to 30 $R_s$ [*Woo and Habbal*, 1999b]. This study has also shown that within the polar coronal hole and quiet Sun the latitudinal density profile at 1.15 $R_s$ is radially preserved with increasing radial distance. We have superimposed the corresponding Mk III pB profiles at 1.15 $R_s$ on the flow speed profiles in Plates 1b and 2b. The January 19 profile in Plate 1b is closest in time to the UVCS measurements of the southern polar coronal hole, while the April 27 profile in Plate 2b is closest in time to the UVCS measurements of the west limb. The vertical lines designated II and III in Plate 1b and III in Plate 2b represent the coronal hole boundaries determined at the solar surface in the plane of the sky from the He I 10830 nm maps obtained from disk observations. These boundaries, demarcating the coronal hole and neighboring quiet Sun regions, are also shown as dashed white lines in Plates 1a and 2a. Consistent with previous studies [*Woo and Habbal*, 1999a, b], the pB profile at 1.15 $R_s$ increases by a factor of 2–3 from the polar coronal hole to the neighboring quiet Sun.

Unlike the radial extension of coronal holes and the quiet Sun, the streamer region is that in which the density profile of the outer corona beyond 5 $R_s$ no longer matches the density profile at 1.15 $R_s$ but exhibits a sharp rise as it departs from the radially preserved inner corona profile at 1.15 $R_s$ [*Woo and Habbal*, 1999b]. The latitudes at which this departure begins define the streamer boundaries and can only be identified in the 1.15 $R_s$ profiles of Plates 1b and 2b if density profiles beyond 5 $R_s$ are also available. While LASCO observes the outer corona, it is not possible to use its measurements because the supporting pylon was located in the quadrant where most of the UVCS measurements took place during January 1997 [*Brueckner et al*., 1995]. Instead, we will use the Mk III profile at 1.74 $R_s$ as a proxy for the density profile beyond 5 $R_s$ to locate the streamer boundary. Although Mk III observes the corona at slightly higher altitudes, we have chosen the profiles at 1.74 $R_s$ because this is the highest altitude before which detection of the streamer boundary may become a problem due to inadequate measurement sensitivity.

We have compared the pB profile of August 11, 1997, at 1.74 $R_s$ with the density profiles on the same day at 1.15 and 5.5 $R_s$ investigated by *Woo and Habbal* [1999b]. Departure between

the 1.15 and 5.5 $R_s$ profiles occurred where the pB level at 1.74 $R_s$ was $100 \times 10^{-10} B_o$ on the east limb and $70 \times 10^{-10} B_o$ on the west limb (where $B_o$ is the pB of disk center). Because of the steep gradient in the pB profile at 1.74 Ro in the range of $70–100 \times 10^{-10} B_o$, the corresponding latitude is relatively insensitive to the pB level (see Plates 1c and 2c), and we choose the level of $100 \times 10^{-10}$ in the 1.74 $R_s$ profile as a proxy for the location of the streamer boundary in the outer corona beyond 5 $R_s$. While the streamer is detected in the 1.74 $R_s$ profile, the tenuous density of the polar coronal hole is not. Thus the radial extension of the polar coronal hole and quiet Sun, observed when more sensitive measurements like those by LASCO white light [*Woo and Habbal*, 1999b] and radio ranging [*Woo and Habbal*, 1999a] are available, is not evident in the 1.15 and 1.74 $R_s$ profiles of Plates 1 and 2.

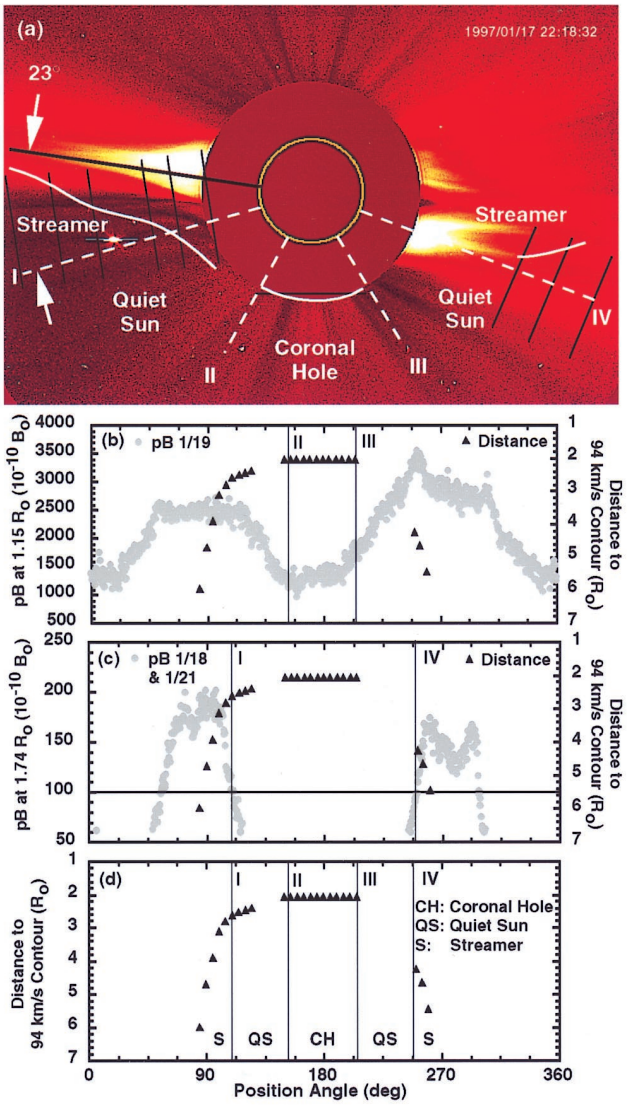


**Plate 1.** Observations during the period of January 17–21, 1997. (a) White light image of the corona taken with the Large-Angle and Spectrometric Coronograph (LASCO) C2 on Solar and Heliospheric Observatory (SOHO) on January 17, 1997. The white contours mark the ratio of the oxygen 1032/1037 line intensities equal to 2 or, equivalently, 94 km $s^{-1}$ [*Habbal et al.*, 1997]. The dashed white lines demarcate the streamer, quiet Sun, and polar coronal hole regions and are shown as vertical lines in Plates 1b–1d. Note that $R_o$ is the same as $R_s$. The profile of radial distance to 94 km $s^{-1}$ contour in Plate 1a is shown in Plates 1b–1d. The Mk III pB profile at 1.15 $R_s$ is combined in Plate 1b, while the Mk III pB profile at 1.74 $R_s$ is combined in Plate 1c. The horizontal line in Plate 1c corresponds to pB = $100 \times 10^{-10} B_o$.

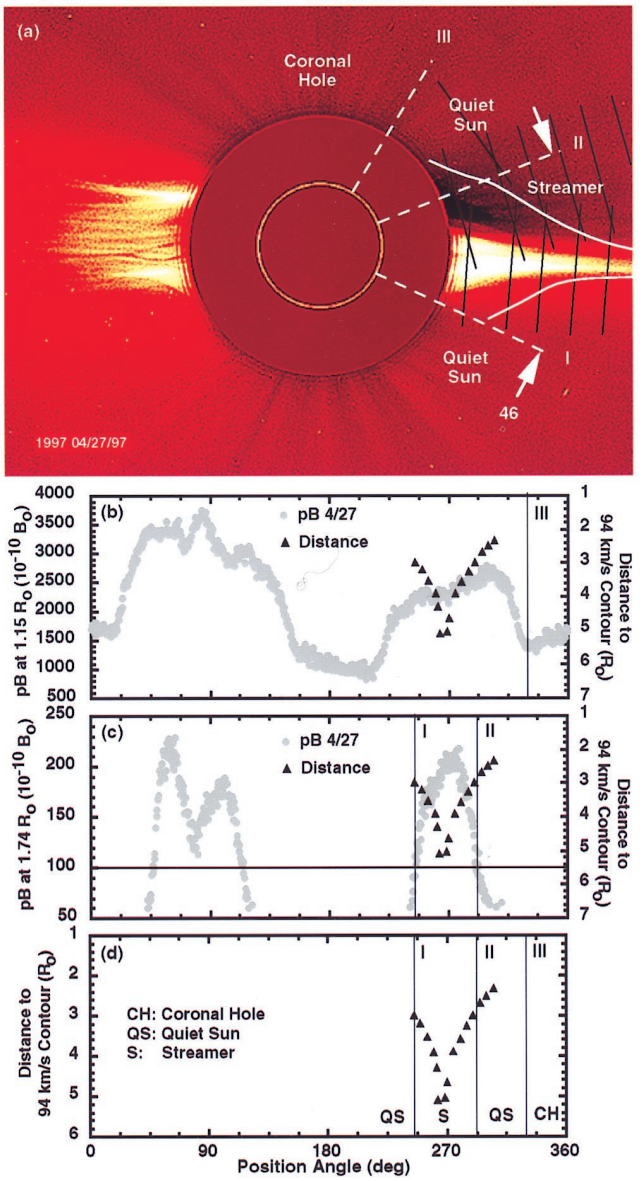


**Plate 2.** Same as Plate 1 except for observations during the period of April 23–27, 1997.

The Mk III pB profiles at 1.74 $R_s$ during the UVCS measurements are shown in Plates 1c and 2c. We have selected the January 18 and 21 profiles for the east and west limb, respectively, in Plate 1c and the April 27 profile for the west limb in Plate 2c because these best match the times of the UVCS measurements of the streamers. The vertical lines designated I and IV in Plates 1b–1d and I and II in Plates 2c–2d have been drawn where pB is $100 \times 10^{-10} B_o$ (the horizontal lines in Plates 1c and 2c indicate this level). Demarcating the streamer and quiet Sun regions, these boundaries are also shown as dashed white lines in Plates 1a and 2a.

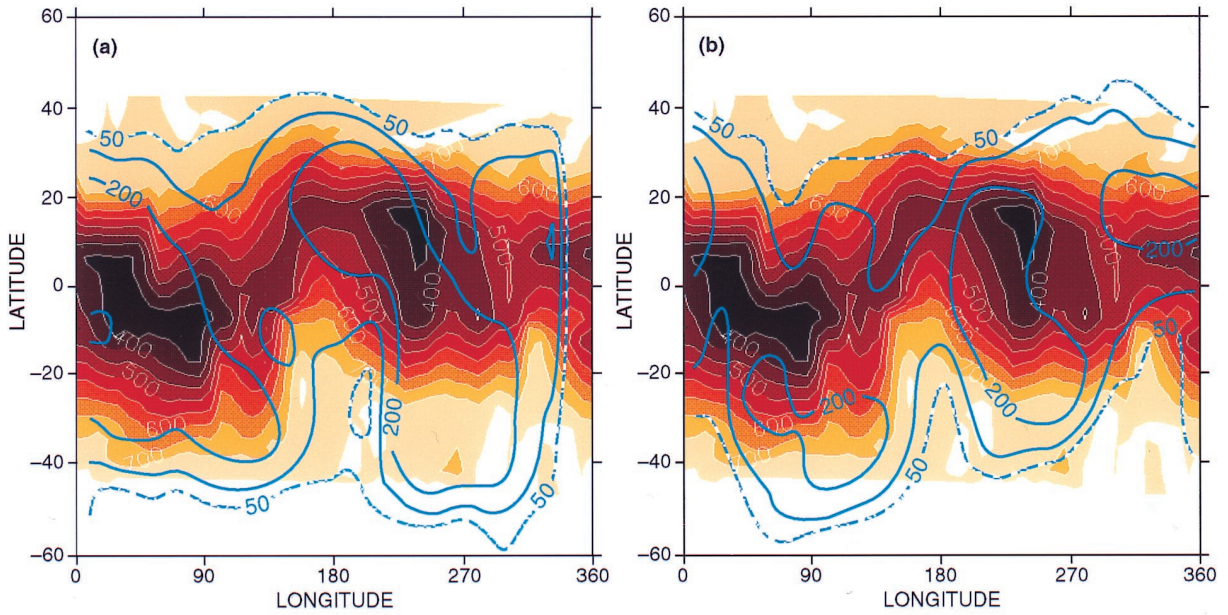


**Plate 3.** (a) Solar wind flow speed contours constructed by *Neugebauer et al.* [1998] from solar wind measurements by Ulysses and Wind during Carrington rotations (CRs) 1891–1895; superimposed is the Mk III synoptic map of pB contours ($10^{-10}\,B_o$) at 1.74 $R_s$ for CR 1893 based on east limb measurements. Note that in all of the Mk III synoptic maps the 100 contour level is that between 50 and 200. (b) Same as Plate 3a except that the pB contours are for CR 1891 and are based on west limb measurements.

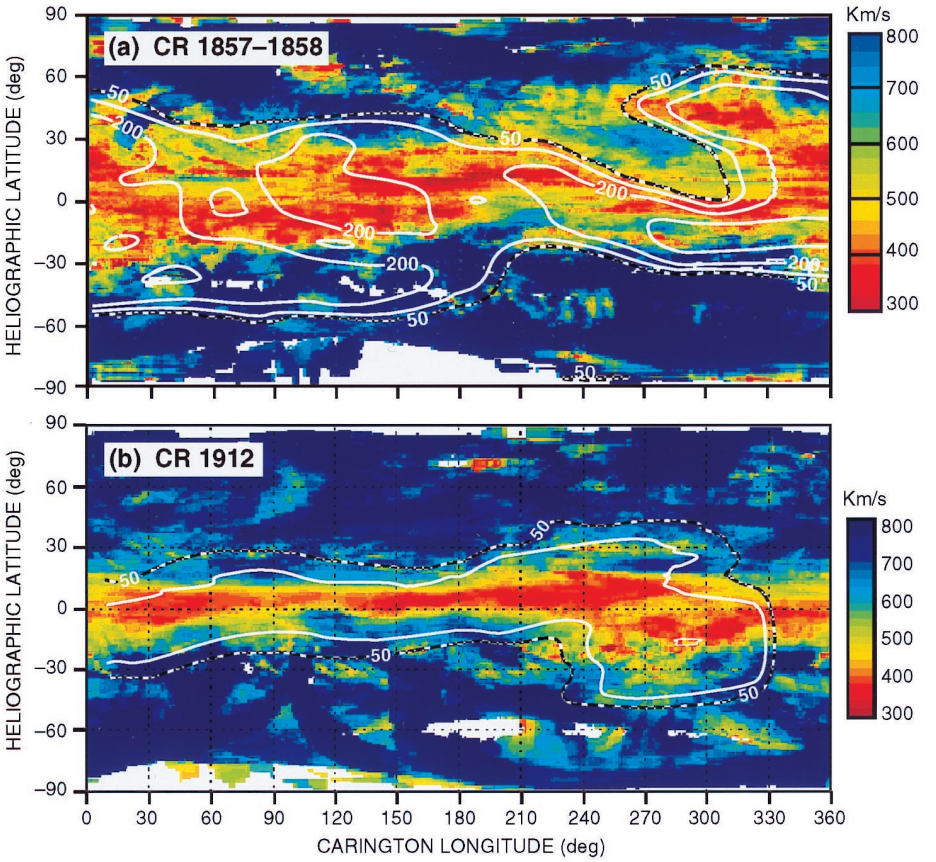


**Plate 4.** (a) Solar wind speed maps determined during CRs 1857–1858 using tomographic reconstruction of interplanetary scintillation (IPS) measurements made with the Nagoya network of radio telescopes in the distance range of 0.3–1.0 AU [*Kojima et al.*, 1998]; superimposed is the Mk III synoptic map of pB contours at 1.74 *Ro* based on west limb data during CR 1857 (b) Same as Plate 4a except that the IPS map is for CR 1912 and the synoptic map of pB at 1.74 $R_s$ is based on east limb data during CR 1912.

### 2.3. Relationship of Flow Speed to Density

The three regions identified from the gradient of the flow speed profiles shown in Plates 1d and 2d coincide with those from the density profiles, with flow speed and density being generally anticorrelated. For instance, the streamer boundary defined in Plate 1c and marking the point at which the density profile of the corona beyond 5 $R_s$ shows a sharp rise when entering the streamer region matches the point at which the flow speed profile declines abruptly while entering the streamer region. When crossing from coronal hole to quiet Sun, density starts to rise steadily, and this also coincides with the beginning of the slight but steady decline of flow speed (see Plate 1b).

There is consistency in the flow speed profiles too. For instance, similarly steep flow speed profiles are found in all of the streamer regions (beyond I and IV in Plate 1d and within I and II in Plate 2d). The well-defined streamer regions in Plate 2a shows an angular extent of 46°, and this is consistent with the 23° extent of one side of the streamer in Plate 1a. Solar wind flow in the quiet Sun is always fast (as indicated by the radial distances between I and II in Plate I and II and III in Plate 2), but it is unmistakably lower than that emanating from the coronal hole. The flow speed measurements of the polar coronal hole and quiet Sun took place at heliocentric distances as far as 3 $R_s$ (between I and II and II and III in Plate 1d and between II and III in Plate 2d). However, latitudinal density profiles following the evolution of structure in the corona have shown that the solar wind extends radially from both the quiet Sun and polar coronal holes starting at 1.15 $R_s$ [*Woo and Habbal*, 1999b]. Furthermore, it is not possible to confuse the polar coronal hole and quiet Sun regions since the simultaneous Mk III measurements show that the polar coronal hole and quiet Sun boundaries (I and II in Plate 1d) are widely separated in latitude. The flow speed measurements presented here therefore provide evidence for the quiet Sun as an additional source of fast solar wind.

One difference between the density and radial distance (and, consequently, flow speed) profiles in Plates 1b–1d and 2b–2d is that the density profiles are at a fixed altitude, while the flow speed profiles are not. Still, when the inverse radial distance is taken as an indicator of flow speed, the flow speed in the quiet Sun region is not more than 25% slower than that in the coronal hole, while in the streamer region it is as much as 65% lower. It is interesting to note that the rise in density from polar coronal hole to quiet Sun is considerably higher (factor of 2 as seen in Plate 1b) than the corresponding drop in flow speed from coronal hole to quiet Sun (at most 25% slower).

## 3. Connecting Fast Solar Wind Observed Beyond 0.3 AU to the Sun

Solar wind measurements by Ulysses during its rapid scan in 1995 near 1.34 AU and by Wind at 1 AU in the ecliptic plane have been used to construct latitude-longitude maps of solar wind flow speed [*Crooker et al*., 1997; *Neugebauer et al*., 1998]. Reproduced in Plate 3 is the map from *Neugebauer et al*. [1998] covering Carrington rotations (CRs) 1891–1895. The 700 km $s^{-1}$ contour marks the beginning of the steep drop in flow speed with decreasing latitude, as measured by Ulysses, and hence represents the approximate low-latitude boundary of the fast wind region.

Superimposed on the Ulysses/Wind solar wind flow maps in Plate 3 are the synoptic contour maps (isophotes) of pB based on the Mk III K-coronameter measurements at 1.74 $R_s$. Two different rotations, CR 1893 based on east limb data (Plate 3a) and CR 1891 based on west limb data (Plate 3b), are shown to reveal the apparent temporal change that took place during the Ulysses measurements. As determined earlier, the pB = $100 \times 10^{-10} B_o$ contour defines the streamer/quiet Sun boundary (I in Plate 1 and II in Plate 2) and hence the low-latitude boundary of the fast wind in the solar corona.

Despite the use of pB as a proxy for velocity the differences between point (Ulysses/Wind) and path-integrated (Mk III) measurements, the disparity in longitudinal probing locations, the assumptions in extrapolation of the solar wind measurements back to the Sun, the evolution of the solar wind with radial distance, and the temporal variations during the five solar rotations, there is similarity in shape and location between the two contours defining the low-latitude boundaries of the fast wind regions in the solar corona (pB = $100 \times 10^{-10} B_o$) and solar wind (flow speed of 700 km $s^{-1}$) in Plate 3. There is better agreement between the pB and solar wind measurements in the Southern Hemisphere in Plate 3b, especially in the longitude range of 180°–360°, because CR 1891 was closer to the time when Ulysses probed the Southern Hemisphere. The coincidence in latitude and longitude between the solar corona and solar wind boundaries means that the fast solar wind regions observed by Ulysses/Wind map radially into the fast wind regions at the Sun.

The flow speed of 700 km $s^{-1}$ was chosen to define the low-latitude boundary of the fast solar wind because it marks the beginning of the steep gradient (drop) in the Ulysses/Wind, flow speed measurements of Plate 3. Similarly, $100 \times 10^{-10} B_o$ corresponds to the level of pB when the gradient of the radial distance profile of Plate 1c steepens sharply. The angular separation between adjacent contours in both flow speed measurements of the solar wind and pB measurements of the corona is small because of these steep gradients. The uncertainties in the locations of the fast wind boundaries in both the solar wind and the solar corona are therefore only several degrees. As evident in the comparisons of Plates 3 and 4, such uncertainties do not affect the conclusion of radial mapping.

Latitude-longitude maps of the contours of flow speed closer to the Sun in the distance range of 0.3–1.0 AU have also been deduced from IPS measurements made by the Nagoya network of radio telescopes [*Kojima et al*., 1998]. Shown in Plate 4a are the Nagoya maps for CRs 1857–1858 in 1992 and in Plate 4b are those for CR 1912 in 1996. These maps show significant changes in the distribution of fast solar wind over the period of 4 years (1992–1996) during the declining phase of the solar cycle. Superimposed on these are the Mk III latitude-longitude maps of pB at 1.74 $R_s$ for CR 1857 on the basis of west limb data and for CR 1912 on the basis of east limb data.

The coincidence between the 700 km $s^{-1}$ boundaries and the Mk III pB = $100 \times 10^{-10} B_o$ contours in Plate 4 is better than that in Plate 3, most likely reflecting the fact that IPS and white light are both path-integrated measurements, that both observe the solar wind off the limb of the Sun, that the IPS observations probe closer to the Sun than those by Ulysses/Wind, and that the observations in Plate 4 cover a period shorter than those in Plate 3 so that temporal variations may be less significant. In the case of CRs 1857–1858 (Plate 4a), there is a notable discrepancy between the pB and IPS contours in the longitudinal range of 60°–210° near latitude −45°. This may be caused by temporal change since source surface magnetic

field maps [*Hoeksema and Scherrer*, 1986] show considerable variation in this region between CRs 1856 and 1857.

As concluded by *Habbal et al*. [1997] and evident within the streamer region of angular extent about 46° in Plate 2, the source of the slowest solar wind is the streamer stalk, with flow speed steadily rising with increasing angular distance from it. In situ solar wind measurements near the ecliptic plane have shown profiles of flow speed as a function of latitudinal separation from the heliospheric current sheet that are similar in shape and angular extent [*Hakamada and Akasofu*, 1981; *Zhao and Hundhausen*, 1981; *Newkirk and Fisk*, 1985; *Bruno et al*., 1986; *Kojima and Kakinuma*, 1990]. This similarity is not surprising as Faraday rotation observations have shown that the streamer stalk encompasses the heliospheric current sheet in the corona [*Woo*, 1997]. The results in Plate 3, however, give more details of this connection.

When *Neugebauer et al*. [1998] added the heliospheric current sheet to the Ulysses solar wind measurements displayed in Plate 3, they pointed out that the band of low-speed solar wind along the heliospheric current sheet was not uniform. The superimposed pB measurements in Plate 3 suggest that this nonuniformity has its origin at the Sun. In spite of evolution with heliocentric distance and despite representing path-integrated measurements the synoptic maps of density at 1.74 $R_s$ clearly discern two regions of enhanced density (and by proxy, depressed flow speed) at the Sun, and these roughly coincide with the two regions of lowest flow speed observed by Ulysses/Wind. The anticorrelation between coronal density and solar wind speed measurements at latitudes lower than 60° has also been identified in other studies based on IPS measurements near solar minimum [*Sime and Rickett*, 1981; *Yokobe et al*., 1999]. Thus not only does the boundary of the fast wind (streamer region) extend approximately radially into interplanetary space, so apparently do the "islands" of dense slow solar wind. Models of the solar wind in which wind speeds are assumed to depend only on the angular distance from the heliospheric current sheet [e.g., *Wang et al*., 1997] would likely be improved if the nonuniformity of peak density and minimum flow speed along the heliospheric current sheet is taken into account.

## 4. Conclusions and Discussion

The measurements described here were made in 1997 when the heliospheric current sheet was relatively flat and the polar coronal hole, quiet Sun, and streamer regions were most isolated from each other in path-integrated measurements. Using inferences of flow speed from ultraviolet spectral line measurements in the inner corona, we have found that the three distinct morphological regions identified earlier in coronal density measurements are reflected in the latitudinal distribution of the flow speed there, with flow speed and density being anticorrelated in general.

Density is lowest and the solar wind is fastest in the polar coronal hole. Beyond the polar coronal hole and in the neighboring quiet Sun, where density rises by a factor of ~2–3, flow speed is still fast, but it is unmistakably lower than that originating from the coronal hole. These observations therefore show that fast wind originates from the quiet Sun as well as from polar coronal holes. Within the streamer region of angular extent about 46°, there is a steady increase in density and a steady decrease in velocity with decreasing angular distance from the streamer stalk.

Reliable pB measurements by the Mk III K-coronameter are limited to regions near the Sun. The radial preservation of the latitudinal density profile at 1.15 $R_s$ demonstrated in earlier coronal studies [*Woo and Habbal*, 1999b] effectively extended the probing range of the Mk III K-coronameter to larger heliocentric distances in the polar coronal hole and quiet Sun regions. The results of this paper add further to the usefulness of the Mk III measurements. First, the global anticorrelation between flow speed and density means that the Mk III density measurements also serve as a proxy for solar wind velocity. Second, by showing that the boundary between the quiet Sun and streamer region corresponds approximately to the pB level of $100 \times 10^{-10}\, B_o$ at 1.74 $R_s$, we have determined a criterion for identifying the fast wind regions in the Mk III measurements. (Since this level was established and demonstrated during low solar activity, its usefulness during high-activity conditions still needs to be explored.) The Mk III K-coronameter therefore provides a framework of measurements not only for identifying the regions of fast solar wind but also for obtaining information on the distribution of both density and flow speed within them. This development is especially significant because Mk III has been imaging the corona essentially continuously since 1980 [*Fisher et al*., 1982], a period that spans nearly two solar cycles.

We have used the Mk III database to identify the global fast wind regions in latitude-longitude maps of coronal density and compared them with corresponding maps of the fast wind regions observed by both in situ and IPS measurements beyond 0.3 AU. The similarity of the fast wind distributions in the inner corona and interplanetary space, between two regions widely separated in heliocentric distances and for solar wind velocities deduced from both path-integrated and point measurements, demonstrates that the fast wind originating from both polar coronal holes and quiet Sun expands radially between Sun and Earth. The issue of whether the expansion of the fast wind is radial or superradial can also be addressed independently on the basis of, for example, the latitudinal variation of density and flow speed observed in interplanetary space. We will report on such studies separately.

Interestingly enough, when *Schwenn et al*. [1978] compared white light measurements at 1.5 $R_s$ with Helios flow speed measurements, they found close correlations between the latitudinal boundaries of fast wind and coronal holes, prompting them to conclude that there was only minor nonradial expansion in latitude beyond 1.5 $R_s$, and to point out that this was in contradiction with the conclusions of *Munro and Jackson* [1977]. The Helios results are similar to those of this paper once it is realized that (1) the contour identified previously as the polar coronal hole boundary in the white light measurements at 1.5 $R_s$ coincides approximately with the boundary of the streamer region and (2) the corona in the polar coronal hole and quiet Sun regions expands radially between 1.15 and 1.5 $R_s$ as shown by *Woo and Habbal* [1999b].

Evidence against a superradially expanding fast solar wind, first provided by radio occultation [*Woo and Habbal*, 1999a] and then white light measurements of the solar corona [*Woo and Habbal*, 1999b], has now been found in solar wind measurements beyond 0.3 AU. Clearly, coronal measurements provide the most compelling evidence for radial expansion of the solar wind since they take place closest to the source region before evolution. The evidence from solar wind measurements is, however, also significant because previous investigations based on solar wind measurements far from the Sun either

assumed or reached the opposite conclusion of this paper: that fast solar wind originates exclusively from coronal holes and that polar coronal holes expand superradially, producing high-speed streams near the solar equator [e.g., *Hundhausen*, 1977; *Sime and Rickett*, 1978; *Kojima and Kakinuma*, 1990; *Rickett and Coles*, 1991; *Bame et al*., 1993; *Gosling et al*., 1995; *Coles*, 1995; *Wang et al*., 1997; *Woch et al*., 1997; *Neugebauer*, 1999; *Breen et al*., 1999]. Although a discussion of these studies is beyond the scope of this paper, it should be pointed out that our investigation is unique. It does not depend on theoretical modeling to estimate interplanetary fields and particles from measurements of the photospheric field in lieu of coronal observations. Instead, it is based entirely on observations that include coronal measurements sensitive enough to define latitudinal density profiles even in the highly tenuous outer corona and flow speed measurements in the corona that reveal the anticorrelation between flow speed and density.

**Acknowledgments.** We thank C. Copeland for expertly producing the plates of this paper, H. Gilbert and A. Lecinski for many useful discussions and for generously providing the Mauna Loa Mk III K-coronameter (operated by NCAR/HAO) data, R. Howard (NRL) for the LASCO images, J. Kohl for the UVCS data, M. Kojima for providing the Nagoya IPS maps and discussion, and M. Neugebauer for providing the original of the Ulysses solar wind speed map. The NSO/Kitt Peak He I 1083 nm data used here were produced cooperatively by NSF/NOAO, NASA/GSFC, and NOAA/SEL. This paper describes research carried out at the Jet Propulsion Laboratory, California Institute of Technology, under a contract with the National Aeronautics and Space Administration. Support for S. R. Habbal was provided by NASA grant NAG5-6215.

Janet G. Luhmann thanks Roberto Bruno and another referee for their assistance in evaluating this paper.

## References

Armstrong, J. W., W. A. Coles, M. Kojima, and B. J. Rickett, Solar wind observations near the Sun, in *The Sun and the Heliosphere in Three Dimensions*, edited by R. G. Marsden, pp. 59–64, D. Reidel, Norwell, Mass., 1986.

Bame, S. J., B. E. Goldstein, J. T. Gosling, J. W. Harvey, D. J. McComas, M. Neugebauer, and J. L. Phillips, Ulysses observations of a recurrent high speed solar wind stream and the heliomagnetic streamer belt, *Geophys. Res. Lett*., *20*, 2323–2326, 1993.

Breen, A. R., Z. Mikic, J. A. Linker, A. J. Lazarus, B. J. Thompson, D. A. Biesecker, P. J. Moran, C. A. Varley, P. J. S. Williams, and A. Lecinski, Interplanetary scintillation measurements of the solar wind during Whole Sun Month: Comparisons with coronal and in situ observations, *J. Geophys. Res*., *104*, 9847–9870, 1999.

Brueckner, G. E., et al., The large angle spectroscopic coronagraph (LASCO), *Solar Phys*., *162*, 357–402, 1995.

Bruno, R., U. Villante, B. Bavassano, R. Schwenn, and F. Mariani, In-situ observations of the latitudinal gradients of the solar wind parameters during 1976 and 1977, *Solar Phys*., *104*, 431–445, 1986.

Coles, W. A., Interplanetary scintillation observations of the high-latitude solar wind, *Space Sci. Rev*., *72*, 211–222, 1995.

Crooker, N. U., A. J. Lazarus, J. L. Phillips, J. T. Steinberg, A. Szabo, R. P. Lepping, and E. J. Smith, Coronal streamer belt asymmetries and seasonal solar wind variations deduced from Wind and Ulysses data, *J. Geophys. Res*., *102*, 4673–4679, 1997.

Ekers, R. D., and L. T. Little, The motion of the solar wind close to the Sun, *Astron. Astrophys*., *10*, 310–316, 1971.

Fisher, R., R. H. Lee, R. M. MacQueen, and A. I. Poland, New Mauna Loa coronagraph systems, *Appl. Opt*., *20*, 1094–1101, 1981.

Fisher, R., C. Garcia, K. Rock, P. Seagraves, and E. Yasukawa, The white light solar corona: An atlas of K-coronameter synoptic charts August 1980–September 1981, *NCAR/TN-199+STR*, Natl. Cent. for Atmos. Res., Boulder, Colo., 1982.

Gosling, J. T., S. J. Bame, W. C. Feldman, D. J. McComas, J. L. Phillips, B. Goldstein, M. Neugebauer, J. Burkepile, A. J. Hundhausen, and L. Acton, The band of solar variability at low heliographic latitudes near solar activity minimum: Plasma results from the Ulysses rapid latitude scan, *Geophys. Res. Lett*., *22*, 3329–3332, 1995.

Grall, R. R., W. A. Coles, M. T. Klinglesmith, A. R. Breen, P. J. S. Williams, J. Markkanen, and R. Esser, Rapid acceleration of the polar solar wind, *Nature*, *379*, 429–432, 1996.

Habbal, S. R., R. Woo, S. Fineschi, R. O'Neal, J. Kohl, G. Noci, and C. Korendyke, Origins of the slow and the ubiquitous fast solar wind, *Astrophys. J*., *489*, L103–L106, 1997.

Hakamada, K., and S. I. Akasofu, A cause of solar wind speed variations observed at 1 AU, *J. Geophys. Res*., *86*, 1290–1298, 1981.

Hoeksema, J. T., and P. H. Scherrer, The solar magnetic field—1976 through 1985, *Rep. UAG-94*, World Data Cent. A for Sol. Terr. Phys., Boulder, Colo., 1986.

Hundhausen, A. J., An interplanetary view of coronal holes, in *Coronal Holes and High Speed Streams*, edited by J. B. Zirker, pp. 225–329, Colo. Assoc. Univ. Press, Boulder, 1977.

Kohl, J., et al., The ultraviolet coronagraph spectrometer for the solar and heliospheric observatory, *Sol. Phys*., *162*, 313–356, 1995.

Kojima, M., and T. Kakinuma, Solar cycle dependence of global distribution of solar wind speed, *Space Sci. Rev*., *53*, 173–222, 1990.

Kojima, M., M. Tokumaru, H. Watanabe, A. Yokobe, K. Asai, B. V. Jackson, and P. L. Hick, Heliospheric tomography using interplanetary scintillation observations, 2, Latitude and heliocentric distance dependence of solar wind structure at 0.1–1 AU, *J. Geophys. Res*., *103*, 1981–1989, 1998.

Krieger, A. S., A. F. Timothy, and E. C. Roelof, A coronal hole and its identification as the source of a high velocity solar wind stream, *Solar Phys*., *29*, 505–525, 1973.

Munro, R. H., and B. V. Jackson, Physical properties of a polar coronal hole from 2 to 5 Ro, *Astrophys. J*., *213*, 874–886, 1977.

Neugebauer, M., The three-dimensional solar wind at solar activity minimum, *Rev. Geophys*., *37*, 107–126, 1999.

Neugebauer, M., and C. W. Snyder, Mariner 2 observations of the solar wind, 1, Average properties, *J. Geophys. Res*., *71*, 4469–4484, 1966.

Neugebauer, M., et al., Spatial structure of the solar wind and comparisons with solar data and models, *J. Geophys. Res*., *103*, 14,587–14,599, 1998.

Newkirk, G., Jr., and L. A. Fisk. Variation of cosmic rays and solar wind properties with respect to the heliospheric current sheet, 1, Five-GeV protons and solar wind speed, *J. Geophys. Res*., *90*, 3391–3414, 1985.

Rickett, B. J., and W. A. Coles, Evolution of the solar wind structure over a solar cycle: Interplanetary scintillation velocity measurements compared with coronal observations, *J. Geophys. Res*., *96*, 1717–1736, 1991.

Schwenn, R., M. D. Montgomery, H. Rosenbauer, H. Miggenrieder, K. H. Mühlhäser, S. J. Bame, W. C. Feldman, and R. T. Hansen, Direct observation of the latitudinal extent of a high-speed stream in the solar wind, *J. Geophys. Res*., *83*, 1011–1017, 1978.

Sime, D. G., and B. J. Rickett, The latitude and longitude structure of the solar wind speed from IPS observations, *J. Geophys. Res*., *83*, 5757–5762, 1978.

Sime, D. G., and B. J. Rickett, Coronal density and the solar wind speed at all latitudes, *J. Geophys. Res*., *86*, 8869–8876, 1981.

Wang, Y.-M, N. R. Sheeley Jr., J. L. Phillips, and B. E. Goldstein, Solar wind stream interactions and the wind speed-expansion factor relationship, *Astrophys. J*., *488*, L51–L54, 1997.

Woch, J., W. I. Axford, B. Wilken, S. Livi, J. Geiss, G. Gloeckler, and R. J. Forsyth, SWICS/Ulysses observations: The three-dimensional structure of the heliosphere in the declining/minimum phase of the solar cycle, *Geophys. Res. Lett*., *24*, 2885–2888, 1997.

Woo, R., Solar wind speed structure in the inner corona at 3–12 Ro, *Geophys. Res. Lett*., *22*, 1393–1396, 1995.

Woo, R., Evidence for the reversal of magnetic field polarity in coronal streamers, *Geophys. Res. Lett*., *24*, 97–100, 1997.

Woo, R., and S. R. Habbal, Multiscale filamentary structures in the solar corona and their implications for the origin and evolution of the solar wind in *Physics of Space Plasmas*, vol. 15, edited by T. Chang and J. R. Jasperse, pp. 351–355, Cent. for Theor. Geo/Cosmo Plasma Phys., Mass. Inst. of Technol., Cambridge, 1998.

Woo, R., and S. R. Habbal, Imprint of the Sun on the solar wind, *Astrophys. J*., *510*, L69–L72, 1999a.

Woo, R., and S. R. Habbal, Radial evolution of density structure in the solar corona, *Geophys. Res. Lett*., *26*, 1793–1796, 1999b.

Woo, R., and S. R. Habbal, A new view of the origin of the solar wing, in *Solar Wind Nine*, edited by S. R. Habbal et al., pp. 71–76, Am. Inst. of Phys., College Park, Md., 1999c.

Woo, R., and J. M. Martin, Source regions of the slow solar wind, *Geophys. Res. Lett*., *24*, 2535–2538, 1997.

Yokobe, A., T. Ohmi, K. Hakamada, M. Kojima, M. Tokumaru, B. V. Jackson, P. P. Hick, and S. Zidowitz, Comparison of solar wind speed with coronagraph data analyzed by tomography, in *Solar Wind Nine*, edited by S. R. Habbal et al., pp. 565–567, Am. Inst. of Phys., College Park, Md., 1999.

Zhao, X. P., and A. J. Hundhausen, Organization of solar wind plasma properties in a tilted, heliomagnetic coordinate system, *J. Geophys. Res*., *86*, 5423–5430, 1981.

Zirker, J. *Coronal Holes and High Speed Streams*, edited by J. B. Zirker, Colo. Assoc. Univ. Press, Boulder, 1977.

S. R. Habbal, Harvard-Smithsonian Center for Astrophysics, 60 Garden Street, Cambridge, MA 02138.

R. Woo, Jet Propulsion Laboratory, California Institute of Technology, 4800 Oak Grove Drive, Pasadena, CA 91109. (richard.woo@jpl.nasa.gov)

(Received July 14, 1999; revised November 5, 1999;
accepted November 5, 1999.)